AD-E000029

NRL Report 8166

12

ADA047420

Fatigue Crack Propagation Resistance of Beta-Annealed Ti-6Al-4V Alloys of Differing Interstitial Oxygen Contents

G. R. Yoder, L. A. Cooley, and T. W. Crooker

Metals Performance Branch
Engineering Materials Division

October 4, 1977

AD No.
DDC FILE COPY

NAVAL RESEARCH LABORATORY
Washington, D.C.

Approved for public release; distribution unlimited

SECURITY CLASSIFICATION OF THIS PAGE (When Data Entered)

REPORT DOCUMENTATION PAGE

READ INSTRUCTIONS BEFORE COMPLETING FORM

1. REPORT NUMBER (14) NRL [redacted]8166	2. GOVT ACCESSION NO.
3. RECIPIENT'S CATALOG NUMBER (9)	
4. TITLE (and Subtitle) (6) FATIGUE CRACK PROPAGATION RESISTANCE OF BETA-ANNEALED Ti-6Al-4V ALLOYS OF DIFFERING INTERSTITIAL OXYGEN CONTENTS.	5. TYPE OF REPORT & PERIOD COVERED Final report on one phase of a continuing NRL Problem
	6. PERFORMING ORG. REPORT NUMBER
7. AUTHOR(s) (10) G. R. Yoder, L. A. Cooley[redacted] T. W. Crooker	8. CONTRACT OR GRANT NUMBER(s) (16) RR02201
9. PERFORMING ORGANIZATION NAME AND ADDRESS Naval Research Laboratory Washington, DC 20375	10. PROGRAM ELEMENT, PROJECT, TASK AREA & WORK UNIT NUMBERS NRL Problem [redacted]M01-24 (17) [redacted]RR 022-01-46
11. CONTROLLING OFFICE NAME AND ADDRESS Office of Naval Research Arlington, VA 22217 (11) 4	12. REPORT DATE Oct[redacted]77
	13. NUMBER OF PAGES 17
14. MONITORING AGENCY NAME & ADDRESS(if different from Controlling Office) (12) 17p.	15. SECURITY CLASS. (of this report) UNCLASSIFIED
	15a. DECLASSIFICATION/DOWNGRADING SCHEDULE

16. DISTRIBUTION STATEMENT (of this Report)

Approved for public release; distribution unlimited

(18) SBIE (19) AD-E000 027

17. DISTRIBUTION STATEMENT (of the abstract entered in Block 20, if different from Report)

18. SUPPLEMENTARY NOTES

19. KEY WORDS (Continue on reverse side if necessary and identify by block number)

Fatigue crack propagation
Titanium alloys
Widmanstätten microstructure
Beta anneal
Oxygen content
Beta grain size
Reversed plastic zone size

20. ABSTRACT (Continue on reverse side if necessary and identify by block number)

Fatigue crack growth rates have been determined for beta-annealed Ti-6Al-4V alloys with respective oxygen contents of 0.06, 0.11, 0.18, and 0.20 weight percent. For each of these alloys, transitional crack growth behavior has been observed which appears to correlate with a critical value of the reversed plastic zone size: the Widmanstätten packet size. Moreover, growth rates below transitional levels order in terms of packet size. The present results suggest that interstitial oxygen content and prior beta grain size significantly affect fatigue crack growth rates through control of the Widmanstätten packet size.

DD FORM 1 JAN 73 1473 EDITION OF 1 NOV 65 IS OBSOLETE S/N 0102-014-6601

SECURITY CLASSIFICATION OF THIS PAGE (When Data Entered)

251 950

CONTENTS

AD NUMBER		*************************	E000029 **********************
FIELD 2:	FLD/GRP(S)		20110 11060
FIELD 3:	ENTRY CLASS		U
FIELD 4:	NTIS PRICES		HC MF
FIELD 5:	SOURCE NAME		NAVAL RESEARCH LAB WASHINGTON D (
FIELD 6:	UNCLASS. TITLE		FATIGUE CRACK PROPAGATION RESIST(OF DIFFERING INTERSTITIAL OXYGEN
FIELD 7:	CLASS. TITLE		
FIELD 8:	TITLE CLASS.		U
FIELD 9:	DESCRIPTIVE NOTE		FINAL REPT.,
FIELD 10:	PERSONAL AUTHORS		YODER,G. R. ;COOLEY,L. A. ;CROOKE
FIELD 11:	REPORT DATE		04 OCT 77
FIELD 12:	PAGINATION		17P
FIELD 13:	SOURCE ACRONYM		
FIELD 14:	REPORT NUMBER		NRL-8166
FIELD 15:	CONTRACT NUMBER		
FIELD 16:	PROJECT NUMBER		RR02201
FIELD 17:	TASK NUMBER		RR0220146
FIELD 18:	MONITOR SOURCE		
FIELD 19:	MONITOR SERIES		
FIELD 20:	REPORT CLASS		U
FIELD 21:	SUPPLEMENTARY NOTE		
FIELD 22:	ALPHA LIMITATIONS		DISTRIBUTION OF DOCUMENT CONTROLL 2628, WASHINGTON, D.C. 20375. THI CATALOGING INFORMATION SUPPLIED B
FIELD 23:	DESCRIPTORS		*FATIGUE(MECHANICS), *TITANIUM AL ANNEALING, OXYGEN, INTERSTITIALS,
FIELD 24:	DESCRIPTOR CLASS.		U
FIELD 25:	IDENTIFIERS		WIDMANSTAETTEN MICROSTRUCTURE, BE
FIELD 26:	IDENTIFIER CLASS.		U
FIELD 27:	ABSTRACT		FATIGUE CRACK GROWTH RATES HAVE B ALLOYS WITH RESPECTIVE OZYGEN CON FOR EACH OF THESE ALLOYS, TRANSIT APPEARS TO CORRELATE WITH A CRITI WIDMANSTAETTEN PACKET SIZE. MOREO IN TERMS OF PACKET SIZE. THE PRES AND PRIOR BETA GRAIN SIZE SIGNIFI CONTROL OF THE WIDMANSTAETTEN PAC
FIELD 28:	ABSTRACT CLASS.		U
FIELD 29:	INITIAL INVENTORY		0
FIELD 30:	ANNOTATION		
FIELD 31:	SPECIAL INDICATOR		0
FIELD 32:	REGRADING CATEGORY		
FIELD 33:	LIMITATION CODES		1 21
FIELD 34:	SOURCE SERIAL		F
FIELD 35:	SOURCE CODE		251950
FIELD 36:	DOCUMENT LOCATION		7
FIELD 37:	CLASSIFIED BY		
FIELD 38:	DECLASSIFIED ON		
FIELD 39:	DOWNGRADED TO CONF.		
FIELD 40:	GEOPOLITICAL CODE		1100
FIELD 41:	SOURCE TYPE CODE		N
FIELD 42:	TAB ISSUE NUMBER		00--00

0029 ************************SCN-- AJJ27L

11060

MF

RESEARCH LAB WASHINGTON D C

UE CRACK PROPAGATION RESISTANCE OF BETA-ANNEALED TI-6AI-4V ALLOYS

FFERING INTERSTITIAL OXYGEN CONTENTS.

REPT.,

.G. R. ;COOLEY,L. A. ;CROOKER ,T. W. ;

T 77

166

D1

D146

IBUTION OF DOCUMENT CONTROLLED BY NAVAL RESEARCH LABORATORY, ATTN: CODE
WASHINGTON, D.C. 20375. THIS DOCUMENT IS NOT AVAILABLE FROM DDC.
OGING INFORMATION SUPPLIED BY NRL.
UE(MECHANICS), *TITANIUM ALLOYS, *CRACK PROPAGATION, MICROSTRUCTURE,
LING, OXYGEN, INTERSTITIALS, GRAIN SIZE, RESISTANCE

NSTAETTEN MICROSTRUCTURE, BETA GRAIN SIZE, PE61153N, WUM0124

UE CRACK GROWTH RATES HAVE BEEN DETERMINED FOR BETA-ANNEALED TI-6AI-4V
S WITH RESPECTIVE OZYGEN CONTENTS OF 0.06, 0.11, 0.18, AND 0.20 WEIGHT PERCENT.
ACH OF THESE ALLOYS, TRANSITIONAL CRACK GROWTH BEHAVIOR HAS BEEN OBSERVED WHICH
RS TO CORRELATE WITH A CRITICAL VALUE OF THE REVERSED PLASTIC ZONE SIZE: THE
NSTAETTEN PACKET SIZE. MOREOVER, GROWTH RATES BELOW TRANSITIONAL LEVELS ORDER
RMS OF PACKET SIZE. THE PRESENT RESULTS SUGGEST THAT INTERSTITIAL OXYGEN CONTENT
RIOR BETA GRAIN SIZE SIGNIFICANTLY AFFECT FATIGUE CRACK GROWTH RATES THROUGH
OL OF THE WIDMANSTAETTEN PACKET SIZE.

0

FATIGUE CRACK PROPAGATION RESISTANCE OF BETA-ANNEALED Ti-6Al-4V ALLOYS OF DIFFERING INTERSTITIAL OXYGEN CONTENTS

INTRODUCTION

Though it is well known that interstitial oxygen can markedly affect the fracture toughness and uniaxial tensile properties of titanium alloys, the influence of oxygen content on fatigue crack propagation resistance in these alloys is poorly understood. Moreover, the limited data available on this subject appear to be in disagreement [1-3]. Reference 1, for instance, reported a reduction in fatigue crack growth rates with increased oxygen content in commercially pure α-titanium alloys. On the other hand, subsequent work with α-titanium alloys, as reported in Ref. 2, indicated the opposite result: an increase in growth rates with increased oxygen content. In harmony with this latter finding, Ref. 3 reported that recrystallization annealed Ti-6Al-4V exhibited increased growth rates with increased oxygen content.

However, no results have been reported to date for the beta-annealed, Widmanstätten microstructure, which has been related to superior fatigue crack propagation resistance in Ti-6Al-4V of commercial purity [3-5]. Accordingly, the purpose of our work is to examine fatigue crack propagation behavior in four beta-annealed Ti-6Al-4V plates with respective oxygen contents of 0.06, 0.11, 0.18, and 0.20 weight percent. For the alloy with 0.20 wt-% oxygen, we reported [5] that fatigue crack growth rates for the α/β-rolled, mill-annealed condition can be reduced by as much as an order of magnitude with a beta anneal, owing primarily to a transition to structure-sensitive crack growth in the Widmanstätten microstructure. We found that the transition corresponds to the point at which the reversed plastic zone attains the average Widmanstätten packet size, with the reduction in growth rates below the transition attributable to crystallographic bifurcation in the Widmanstätten packets.

MATERIALS AND PROCEDURES

The alloys studied were received in the form of rolled plate, with chemical analyses as given in Table 1. Each alloy was subjected to the following beta anneal [3]: 0.5 hr at 1038°C, cooled to room temperature plus 2 hr at 732°C, cooled to room temperature. This heat treatment was performed in a vacuum furnace, with cooling accomplished in a helium atmosphere at a rate which approximates that in air.

Metallographic samples of each of the resultant Widmanstätten microstructures were polished and etched with Kroll's reagent. From these, some 190 linear intercept measurements of prior beta grain size (l_β) were made for each alloy, 475 for the Widmanstätten packet size (l_{WP}) and 600 for the alpha grain size (l_α); a minimum of four photomicrographs was used in each case. Cumulative frequency distributions for l_β and l_{WP} are exhibited in

Manuscript submitted August 16, 1977.

Table 1 — Chemical Analyses

Alloy	Content (wt-%)							
	O	Al	V	Fe	N	C	H	Al*
1	0.06	6.0	4.1	0.05	0.008	0.023	0.0050	7.0
2	0.11	6.1	4.0	0.18	0.009	0.02	0.0069	7.6
3	0.18	6.6	4.4	0.20	0.014	0.02	0.0058	8.[illegible]
4	0.20	6.7	4.3	0.10	0.011	0.03	0.0060	9.2

Note: Al* is the aluminum equivalent [6,7]: $Al^* = Al + \frac{Sn}{3} + \frac{Zr}{6} + 10\,(O + C + 2N)$.

Fig. 1, together with mean values ($\bar{l}_\beta$, $\bar{l}_{WP}$) for each alloy. Figure 2a illustrates the contrast in l_β for alloys 3 and 4, and Fig. 2b illustrates the contrast in l_{WP} for alloys 1 and 3. Widmanstätten packet sizes range from 17 μm for alloy 1 to 38 μm for alloy 3. Figure 1 shows that one pair of these alloys (alloys 2 and 3) exhibits values of $\bar{l}_\beta$ which are substantially larger than for the other pair (alloys 1 and 4).

Fatigue crack growth rates (da/dN) were determined in ambient air from compact tension specimens of 25.4-mm thickness, *TL* crack orientation [8], half-height to width ratio of $h/W = 0.486$, and crack length in the range $0.26 \leq a/W \leq 0.62$. The stress-intensity (K) calibration for the specimen is given in Ref. 9. For each of the four alloys, at least two specimens were subjected to cyclic tension-to-tension loading with a haversine waveform, a frequency of 5 Hz, and a load ratio $R = P_{min}/P_{max} = 0.1$. The amplitude of loading, though held constant throughout the growth rate test of a given specimen, was different for duplicate specimens, so that data could be generated over different, yet overlapping spectra of stress-intensity range (ΔK). Crack lengths were measured optically on both faces at 15 X with Gaertner traveling microscopes.

Tests for fracture toughness (K_{Ic}) were also made from these compact tension specimens, in accord with *ASTM* Method E399-74. Tensile properties were determined for the *T* and *L* orientations from standard 12.8-mm-diameter specimens of 50.8-mm gage length. These mechanical properties are given in Table 2.

RESULTS AND ANALYSIS

Fatigue Crack Propagation: Transitional Behavior

Cyclic crack growth rates for alloys 1 through 4 are plotted logarithmically as a function of stress-intensity range in Figs. 3a through 3d respectively. The crack growth behavior of each of the four alloys is distinguished by a clearly defined transition point (indicated by "T" in each figure). At these points the slope or exponent in the growth rate power law [10]

$$da/dN = C(\Delta K)^m \tag{1}$$

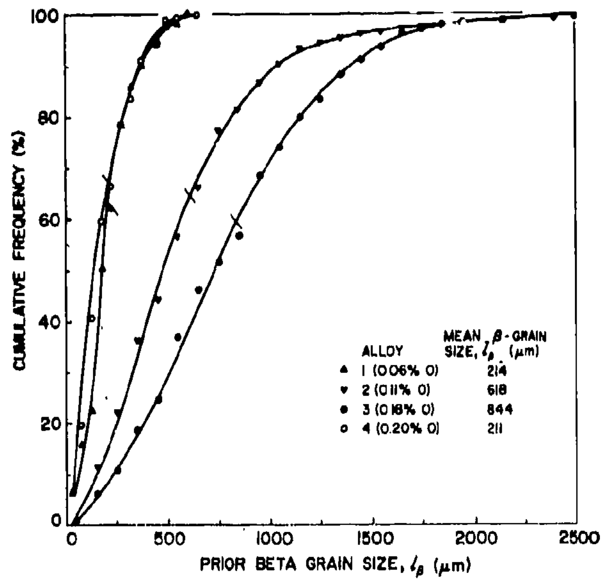

(a) Prior beta grain size

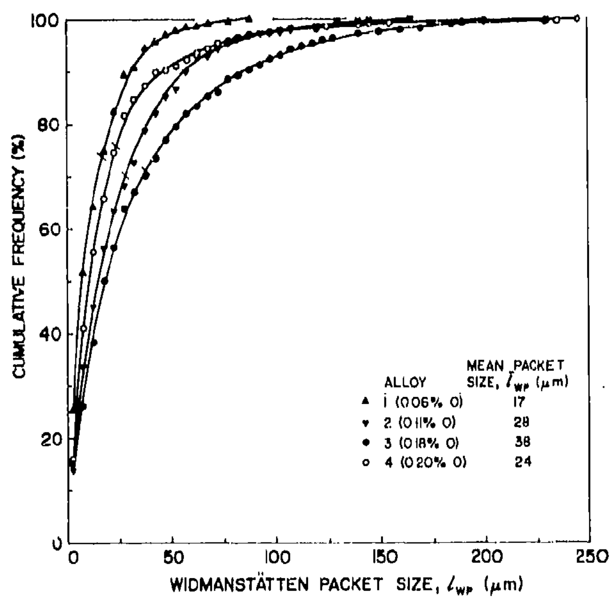

(b) Widmanstätten packet size

Fig. 1 — Cumulative frequency distributions (The slash mark on each curve indicates the mean value.)

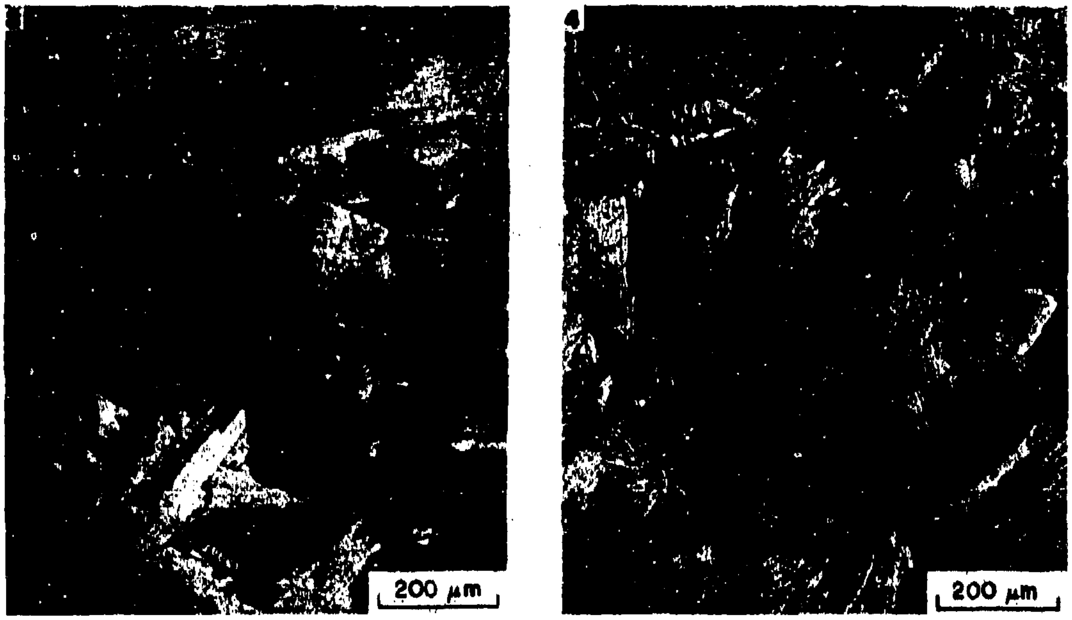

Fig. 2a — Photomicrographs to illustrate contrast in prior beta grain size in alloy 3 (left) and alloy 4 (right)

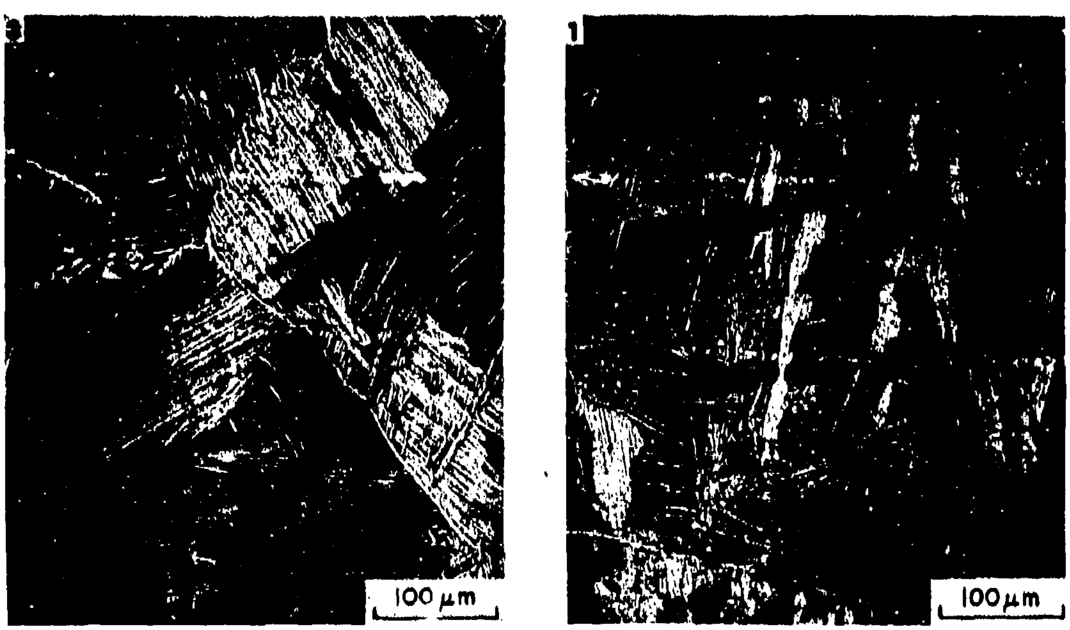

Fig. 2b — Photomicrographs to illustrate contrast in Widmanstätten packet size in alloy 3 (left) and alloy 1 (right)

Table 2 — Mechanical Properties

Alloy No.	Alloy Wt-% Oxygen	Orientation	0.2% Yield Strength σ_y (MPa)	Tensile Strength σ_{uts} (MPa)	Young's Modulus E (GPa)	Reduction in Area (%)	Elongation* (%)	Fracture Toughness K_{Ic} ($MPa \cdot m^{1/2}$)
1	0.06	TL, T	740	818	115	34	10	–
		LT, L	772	829	115	26	10	–
2	0.11	TL, T	772	869	118	19	10	98†
		LT, L	797	867	117	17	8	–
3	0.18	TL, T	818	906	120	13	8	99†
		LT, L	841	931	117	12	8	–
4	0.20	TL, T	869	958	117	16	11	87
		LT, L	892	960	119	23	16	–

*50.8-mm gage length
†Invalid according to ASTM E399-74

changes by approximately a factor of 2. Transitional values of stress-intensity range (ΔK_T) vary from 18 $MPa \cdot m^{1/2}$ for alloy 1 to 27 $MPa \cdot m^{1/2}$ for alloy 3, as noted in Table 3.

Correlation Between Reversed Plastic Zone and Microstructural Dimensions—The transitional behavior of alloy 4 that we reported elsewhere [5] was attributed to a change from microstructurally sensitive crack growth below the transition to microstructurally insensitive crack growth above the transition; moreover, it was found that the transition corresponded to the point at which the reversed plastic zone size [11-13]

$$r_y^c = 0.132 \left(\frac{\Delta K}{2\sigma_y}\right)^2 \tag{2}$$

attained the average Widmanstätten packet size. The data in Table 3 indicate that this is true also for alloys 1 through 3. In this table, microstructural dimensions are compared to the reversed plastic zone size at the transition point ($[r_y^c]_T$), the latter being calculated through Eq. (2), with σ_y and ΔK_T taken from Tables 2 and 3 respectively. For each of the four alloys, the computed value of $[r_y^c]_T$ agrees well with the respective Widmanstätten packet size; values of $\bar{l}_\beta$ are approximately an order of magnitude larger than $[r_y^c]_T$, and values of $\bar{l}_\alpha$ are approximately an order of magnitude smaller.

Structure-Sensitive, Crystallographic Bifurcation ($\Delta K \leqslant \Delta K_T$)—The similarity in behavior of the four alloys is further illustrated by crack-path sectioning normal to the fracture surface. Below their respective transition points, alloys 1 through 3 exhibit crystallographic bifurcation in the Widmanstätten packets similar to that we noted previously in alloy 4 [5]. Thus within packets that border the Mode I crack plane, multiple parallel cracks appear with a distinct relation to the orientation of α-phase platelets, as illustrated in Fig. 4. The reduction in growth rates exhibited below the transition points for all four alloys is therefore attributable to this bifurcation, which serves to reduce the effective ΔK (and thus da/dN) by dispersing the strain field energy of the macroscopic crack among multiple crack tips.

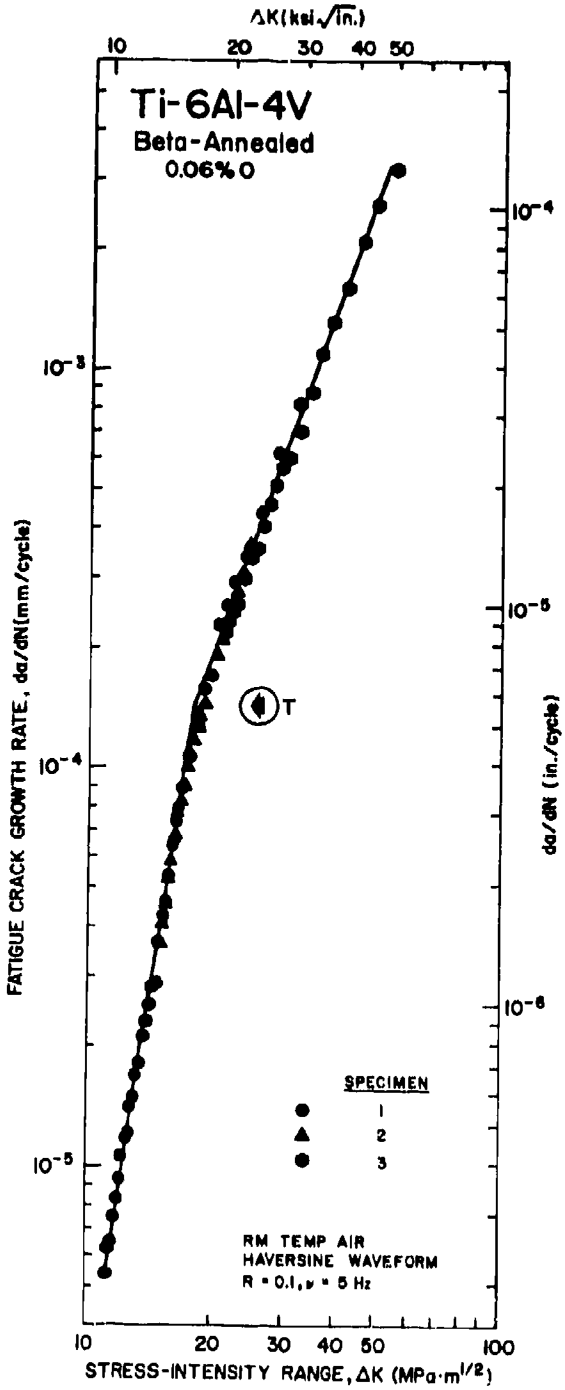

Fig. 3a — Fatigue crack growth rates for alloy 1

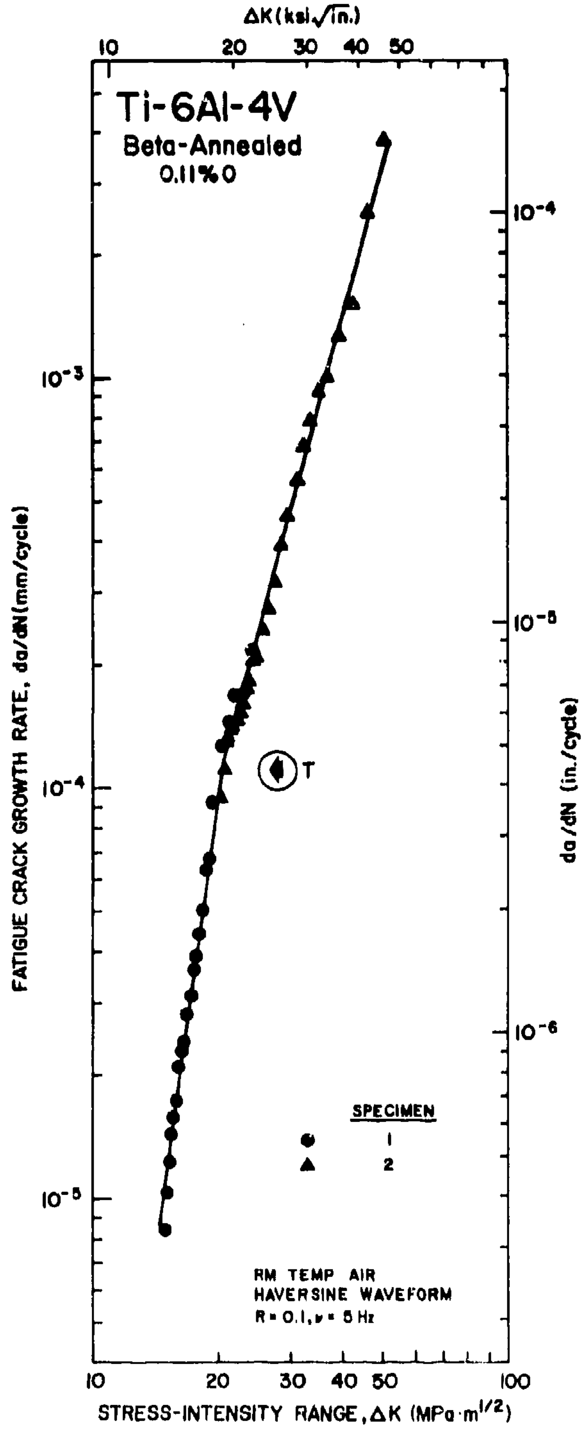

Fig. 3b — Fatigue crack growth rates for alloy 2

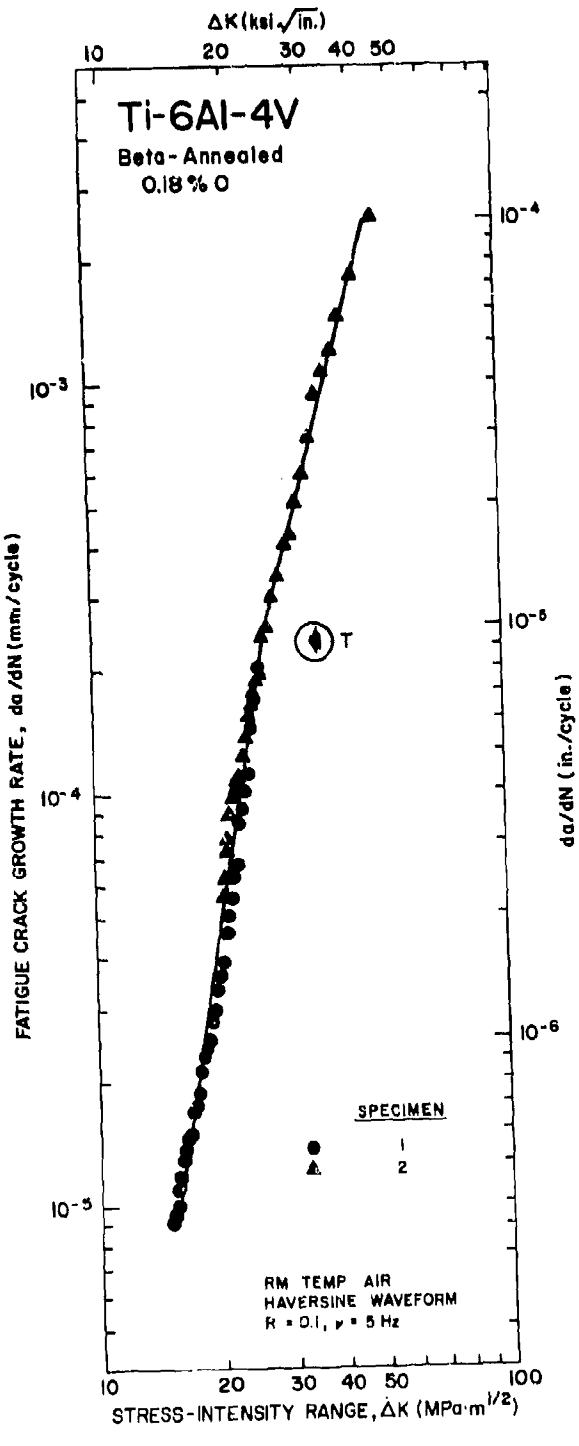

Fig. 3c — Fatigue crack growth rates for alloy 3

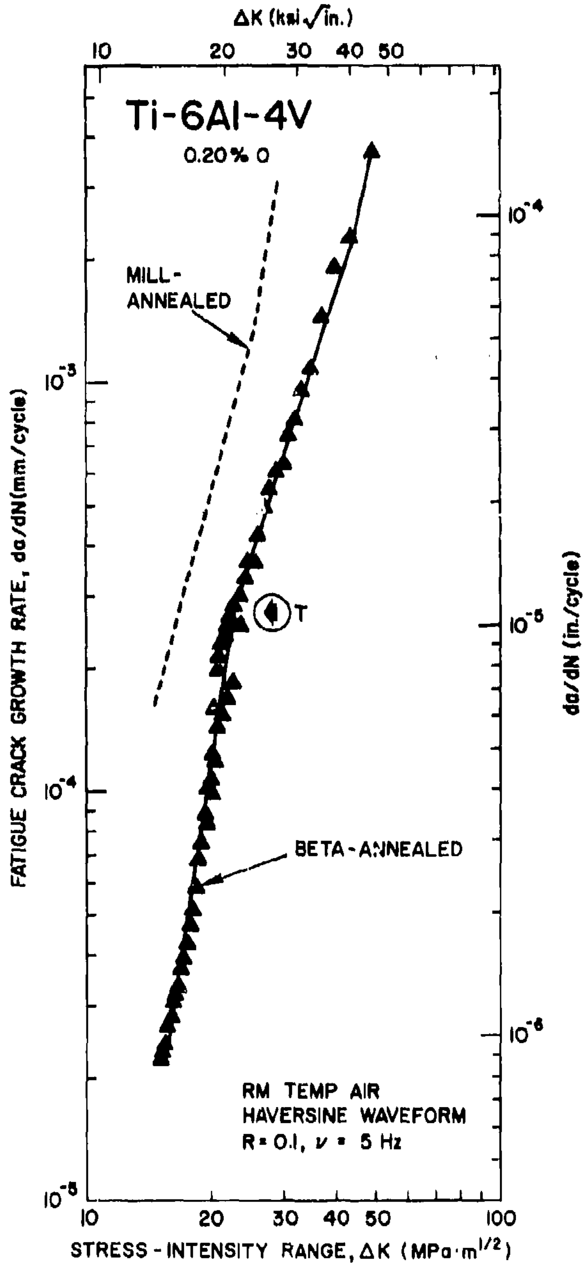

Fig. 3d — Fatigue crack growth rates for alloy 4

Table 3 — Comparison of Transitional Reversed Plastic Zone Size to Microstructural Dimensions

Alloy		Transitional Stress-Intensity Range, ΔK_T ($MPa \cdot m^{1/2}$)	Transitional Reversed Plastic Zone Size, $[r_y^c]_T$ (μm)	Microstructural Dimensions (μm)		
No.	Wt-% Oxygen			$\bar{\ell}_\alpha$	$\bar{\ell}_{WP}$	$\bar{\ell}_\beta$
1	(0.06)	18	19	2	17	214
2	(0.11)	20	23	3	28	618
3	(0.18)	27	35	2	38	844
4	(0.20)	23	23	3	24	211

Comparison of Alloy Crack Propagation Rates ($\Delta K < \Delta K_T$): A 5-Fold Difference

The trend lines drawn through the data points in Fig. 3 are redrawn in Fig. 5 to facilitate comparison of growth rates for the four alloys.

Widmanstätten Packet Size: Key to Reduced Growth Rates—Figure 5 shows that subtransitional crack growth rates order on the basis of Widmanstätten packet size, such that *da/dN decreases* with *increasing* $\bar{l}_{WP}$. For example, at $\Delta K \approx 16$ $MPa \cdot m^{1/2}$, da/dN is about 5 times less for alloy 3 ($\bar{l}_{WP} = 38$ μm) than for alloy 1 ($\bar{l}_{WP} = 17$ μm). Such behavior may be explained on the premise that, with increasing $\bar{l}_{WP}$, the strain-field energy of the macroscopic crack can be spread over increased volumes of material in the crack tip region, thereby further reducing the effective ΔK (and thus da/dN). This presumes that the bifurcation can extend to the boundaries of Widmanstätten packets that border the Mode I plane (or possibly to some lesser dimension related to the maximum plastic zone size).

Effects of Oxygen Content and Prior Beta Grain Size—Further analysis of subtransitional crack growth rates in Fig. 5 leads to the tentative conclusion that interstitial oxygen content, as well as prior beta grain size, significantly affects fatigue crack propagation rates by controlling the subsequent Widmanstätten packet size which develops upon cooling from the beta phase field. Clearly da/dN does not order on the basis of interstitial oxygen content alone (when all four alloys are considered), but if the alloys are paired on the basis of similar prior beta grain size—alloys 1 and 4 ($\bar{l}_\beta = 214$ μm and 211 μm respectively) vs alloys 2 and 3 ($\bar{l}_\beta = 618$ μm and 844 μm respectively)—then the pair with the greater $\bar{l}_\beta$ exhibits the lower growth rates. Yet within each pair the alloy with greater oxygen content exhibits the lower growth rates. Each of these effects is plausible when considered in terms of the transformation kinetics of the $\beta \rightarrow \alpha$ transformation: An increase in $\bar{l}_\beta$ could be expected to reduce the α-phase nucleation rate and thereby serve to increase $\bar{l}_{WP}$, if it is assumed that nucleation occurs primarily at the grain boundaries [14]. Moreover, increased oxygen content could be expected to reduce the α-phase nucleation rate and to enhance the growth rate

(a) Alloy 1 ($\Delta K < \Delta K_T$)

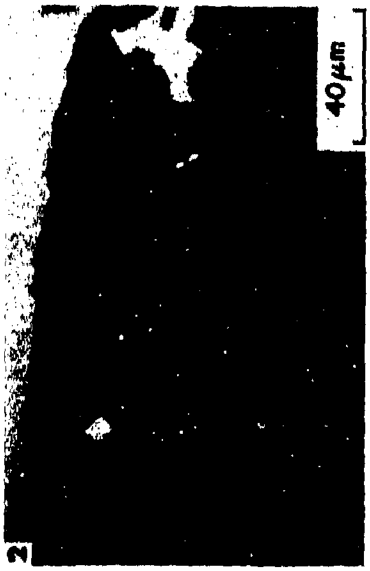

(b) Alloy 2 ($\Delta K \approx \Delta K_T$)

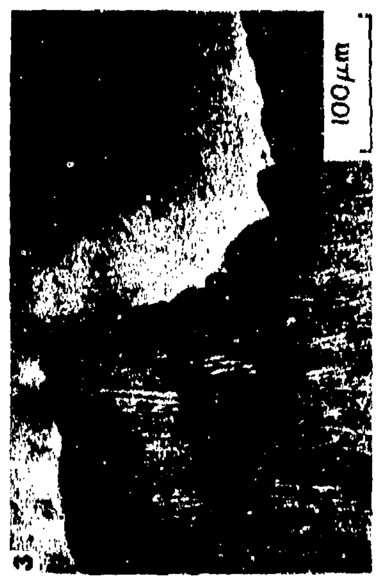

(c) Alloy 3 ($\Delta K < \Delta K_T$)

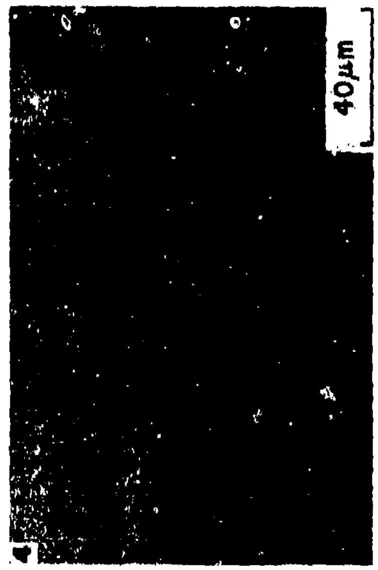

(d) Alloy 4 ($\Delta K < \Delta K_T$)

Fig. 4 — Metallographic crack-path sections

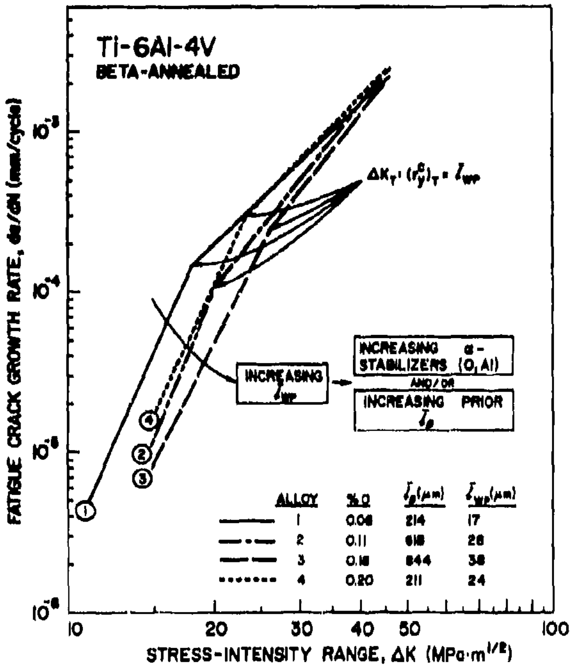

Fig. 5 — Comparison of fatigue crack propagation resistance of alloys 1 through 4

and thus also to promote an increase in $\bar{l}_{WP}$ through a shift in the time-temperature-transformation (TTT) curves to higher temperature and/or lesser time [14,15]. Such a shift with increased oxygen content has been reported by DeLazaro and Rostoker [16] for Ti-11Mo alloys and by Polkin and Kasparova [17] for Ti-3Al-7Mo-11Cr alloys. We are unaware of any such data for the Ti-6Al-4V system.

DISCUSSION

From Table 1, as the oxygen content increases from alloy 1 to alloy 4, so does the aluminum content and the α-phase stabilizer content as given by the aluminum equivalent, Al*. Consequently the relative effects of oxygen content on the one hand and of the remainder of the α-phase stabilizer content on the other would appear to be indeterminate in our work. Therefore it is perhaps appropriate to extend the effect attributed to interstitial oxygen in the preceding section to include the total α-phase stabilizer content: The Widmanstätten packet size increases (and thus da/dN decreases) with increasing α-phase stabilizer content. (The converse effect, namely increasing the β-phase stabilizer content to reduce the Widmanstätten packet size, has recently been reported by Chesnutt, Rhodes, and Williams [18].)

From Table 2, alloys 1 through 4 each exhibit values of Young's modulus (E) which are approximately the same for the T and L directions. This may be taken as evidence that the beta anneal has served to equilibrate any preferred orientation of basal planes (which may have existed prior to the anneal) relative to the T and L directions [19-21]. Consequently the fatigue crack propagation behavior observed for the TL crack orientation in alloys 1 through 4 would also be anticipated for the LT orientation.

CONCLUSIONS

- In the conventional logarithmic plot of fatigue crack growth rate (da/dN) vs stress-intensity range (ΔK), each of the four alloys exhibited a significant change in slope at ΔK_T, a transition point at which the reversed plastic zone appears to attain the average Widmanstätten packet size, $\bar{l}_{WP}$.

- For $\Delta K < \Delta K_T$, a crystallographic bifurcation of the Widmanstätten packets occurs, which is responsible for the markedly lower growth rates below ΔK_T.

- Comparison of alloys indicates that *the larger the average Widmanstätten packet size, the lower the fatigue crack growth rates;* a 5-fold difference in da/dN is observed between the most and least resistant of the four alloys.

- The influence of interstitial oxygen (or α-phase stabilizer content), as well as prior beta grain size ($\bar{l}_\beta$), on fatigue crack propagation resistance appears to be indirect but important, namely to control the size of the average Widmanstätten packet which forms upon cooling from above the beta transus.

ACKNOWLEDGMENTS

We gratefully acknowledge the experimental assistance of G. W. Jackson, M. L. Cigledy, C. R. Forsht and T. R. Harrison.

REFERENCES

1. J. L. Robinson and C. J. Beevers, Met. Sci. 7, 153-159 (1973).
2. A. W. Thompson, J. D. Frandsen, and J. C. Williams, Met. Sci. 9, 46-48 (1975).
3. M. J. Harrigan, M. P. Kaplan, and A. W. Sommer, pp. 225-254 in *Fracture Prevention and Control,* D. W. Hoeppner, editor, Mater./Metalwork. Tech. Ser., No. 3, American Society for Metals, Metals Park, Ohio, 1974.
4. N. E. Paton, J. C. Williams, J. C. Chesnutt, and A. W. Thompson, pp. 4-1 to 4-14, in *AGARD Conference Proceedings 185,* 1976 (available from National Technical Information Service, Springfield, Virginia).
5. G. R. Yoder, L. A. Cooley, and T. W. Crooker, "Observations on Microstructurally Sensitive Fatigue Crack Growth in a Widmanstätten Ti-6Al-4V Alloy," Met. Trans. A (in press).
6. H. W. Rosenberg, pp. 851-859 in *The Science, Technology and Application of Titanium,* R.I. Jaffee and N. E. Promisel, editors, Pergamon Press, Oxford 1970.

7. R. I. Jaffee, pp. 1665-1693 in *Titanium Science and Technology*, Vol. 3, R. I. Jaffee and H. M. Burte, editors, Plenum Press, New York, 1973.

8. R. J. Goode, Mater. Res. Stand. *12*, (No. 9) 31-32 (1972).

9. W. G. Clark, Jr., and S. J. Hudak, Jr., J. Test. Eval. *3*, 454-476 (1975).

10. P. C. Paris and F. Erdogan, Trans. ASME, J. Basic Eng., Series D, *85*, 528-533 (1963).

11. P. C. Paris, pp. 107-127 in *Fatigue-An Interdisciplinary Approach*, J. J. Burke, N. L. Reed, and V. Weiss, editors, Syracuse University Press, 1964.

12. J. R. Rice, pp. 247-309 in *Fatigue Crack Propagation*, ASTM STP 415, American Society for Testing and Materials, Philadelphia, 1967.

13. G. T. Hahn, R. G. Hoagland, and A. R. Rosenfield, Met. Trans. *3*, 1189-1202 (1972).

14. R. I. Jaffee, pp. 65-163 in *Progress in Metal Physics*, Vol. 7, B. Chalmers and R. King, editors, Pergamon Press, New York, 1958.

15. M. K. McQuillan, Met. Rev. *8*, 41-104 (1963).

16. D. J. DeLazaro and W. Rostoker, Acta Met. *1*, 674-678 (1953).

17. I. S. Polkin and O. V. Kasparova, pp. 1521-1534 in *Titanium Science and Technology*, Vol. 3, R. I. Jaffee and H. M. Burte, editors, Plenum Press, New York, 1973.

18. J. C. Chesnutt, C. G. Rhodes, and J. C. Williams, pp. 99-138 in *Fractography—Microscopic Cracking Processes*, C. D. Beachem and W. R. Warke, editors, ASTM STP 600, American Society for Testing and Materials, Philadelphia, 1976.

19. A. W. Bowen, Mater. Sci. Eng. *29*, 19-28 (1977).

20. M. J. Harrigan, A. W. Sommer, P. G. Reimers, and G. A. Alers, pp. 1297-1320 in *Titanium Science and Technology*, Vol. 2, R. I. Jaffee and H. M. Burte, editors, TMS-AIME, Plenum Press, New York, 1973.

21. F. Larson and A. Zarkades, Report MCIC-74-20, Metals and Ceramics Information Center, Battelle-Columbus Laboratories, Columbus, Ohio, June 1974.